

# Heuristic Optimization of a Dual Thermal Actuator Amplitude

Víctor Omark Méndez Ferreira<sup>a</sup>

Prof. Y.C. Lee MEMS 2

<sup>a</sup>Department of Mechanical Engineering, University of Colorado, Boulder, CO 80309-0427, USA

## Abstract

In this paper different designs of dual thermal actuator to be fabricated using surface micromachine techniques (MUMPs), and its characteristics are presented. The novel actuator enables motion in two planes simultaneously by combining a lateral thermoactuator and a bimorph actuator. Expansion of the elements by either a difference in current density between two elements or thermal coefficient mismatch is the mechanism of actuation. Analytical and finite element models were developed to predict and optimize its amplitude of motion. Also, the variation of amplitude related to the actuator's geometry was investigated.

*Keywords: MEMS; Thermoactuator; Bimorph; Finite element analysis*

## Introduction & Definition

Thermal actuators have the ability to provide large deflections and great force compared to electrostatic actuators. Previous work has been done in lateral [5] and bimorph thermal actuators [6], both having displacements in one plane only, z and y or x respectively. Despite the advantages and performance of these devices, there is a need for an actuator that enables motion in two planes. A Dual Thermal Actuator (DTA) combines a lateral and a bimorph thermal actuator (figure 1) to allow for specific patterns of displacement in two planes. A heuristic optimization of this device considers seven different designs in which the ratio of one actuator becomes larger related to the other in each design. With an understanding of how geometric configurations and stiffness of the structure affect its displacement in vertical and horizontal planes, this device can be optimized for maximum amplitude for a given voltage.

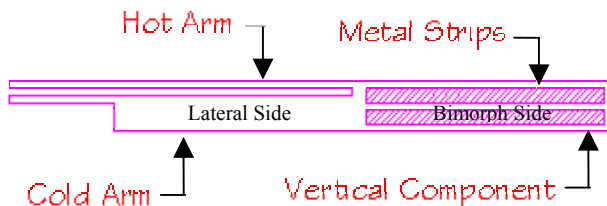


Fig. 1. Proposed Dual Thermoactuator to be fabricated in MUMPs process.

The optimized model will be particularly useful to investigate the performance of two in-series thermal actuators depending on its volume distribution. Also, fundamental insights on coupling design considerations can be obtained. Future applications for this actuator include micromanipulation, to bridge the gap between micro-

technologies and nano-technologies [7], and development of microrobots [8]. This DTA is one more step towards the fabrication of microrobots because of its suitable bi-plane range of motion.

## Synthesis & Device Configuration

A MUMPS thermoactuator is designed for bi-plane actuation motion. The structure resembles a lateral thermoactuator with a bimorph thermal actuator fused at its free end, as shown in Fig1.

In MEMS, two movable parts usually have to be fused together instead of been joined by some hinge or mechanism that allows them to rotate. The fabrication of connections or movable joints using surface macromachining techniques is very difficult due to the nature of its planar deposition process. Also, fabrication process (MUMPs) doesn't provide many structural layers that can be used to create complex parts. As a consequence, when two actuators or movable parts are fused together they tend to restrain the motion of one over the other. This effect of motion restriction of a movable part over another one is known as a coupling effect. To avoid this coupling effect, a lateral and a bimorph thermal actuator were combined in series deliver maximum amplitude in the vertical and horizontal direction.

This simple dual thermoactuator is the combination of a lateral and a bimorph thermal actuator with different rectangular conductive arms, widths and materials (figure 1). A lateral thermoactuator consists of two parallel conductive arms with different dimensions, length and width. The cross sectional area of one arm, called the hot

arm, is significantly smaller than the cross sectional area of the second arm, the cold arm [5]. Its actuation mechanism relies on the fact that current density in the hot arm is higher, resulting in a higher thermal expansion than the cold arm. The difference in thermal expansion is due to ohmic heating in both arms when the same current flows through them. Thus, a lateral deflection (parallel to xy plane) occurs at the tip of the thermal actuator where both arms are connected. A bimorph thermoactuator moves by means of using two materials of different thermal coefficient expansion. When there is a change in temperature, one element will expand more than the other resulting in a displacement at one of the ends of this actuator.

Lateral thermoactuators have typical dimensions of 100 - 200  $\mu\text{m}$  long, 10 - 18  $\mu\text{m}$  wide with deflections of 10 - 15  $\mu\text{m}$  at the tip [5]. Bimorph thermal actuators deflection relies on different thermal coefficients of expansion mismatch between two different staked layers of materials [6]. Due to the previous statement and the simple geometry of the bimorph part of this device, its geometric parameters were easily defined. On the other hand, the dimensions for the lateral actuator side were obtained from the empirical analysis of Comtois, Bright and Phipps [5]. Thus, this device has dimensions of 14 x 200 micron, with height determined by the deposition process (MUMPs), and an initial length ratio of 25% between the lateral and bimetal parts.

### Analytical Modeling

The analytical approach taken considers small deflections angles of the tip related to the original position of the bimorph side and the thermal actuator side. Since actuation motion of this device happens individually in two different planes it is possible to break it down into two devices and analyze it. Whereas the lateral thermal actuator side of the DTA is the one that is anchored to the substrate, the analysis will begin considering this side first.

As previously discussed, the hot arm of a thermal actuator expands significantly more than the cold arm. Therefore, we can assume that the expansion of the cold arm can be neglected compared to the expansion of the hot arm. For a simplified geometry of the thermal actuator that does not take into account stiffness of its different elements, the new length of the hot arm due to thermal expansion is;

$$L_{new} = \int_0^{L_h} [1 + \alpha(T(x) - T_0)] dx \quad (1)$$

derived in [9]. Here  $T(x)$  is the temperature distribution along the hot arm,  $T_0$  is initial temperature at the anchored ends,  $L_h$  is the initial length of the hot arm, and  $\alpha$  is the

thermal coefficient expansion of the material, assumed to be constant.

The temperature distribution along the hot arm can be determined by heat transfer analysis of an idealized DTA. Figure 2 shows a simple layout of four interconnected uniform elements that better represent the dual thermoactuator geometry. The nodes a, b, and c are connection points between elements at which the temperature and heat transferred are assumed to be same.

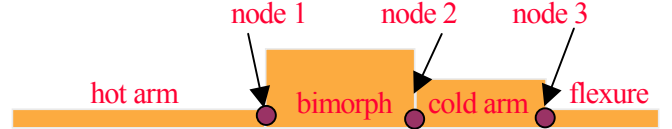


Fig 2. Idealized interconnected uniform elements of a DTA for heat transfer analysis.

For simplicity purpose in deriving this model steady-state condition and non-significant self-heating between elements are assumed. The general heat equation of an element of simple geometry can be derived from the first law of thermodynamics and Fourier's law [9]. This is;

$$\frac{d^2T}{dx^2} + \beta - \gamma^2(T - T_\infty) = 0 \quad (2)$$

where the first term on the left side is the temperature distribution along the element,  $\beta$  is the internal heat generation, and the third term is the surface flux. The ohmic heating is intrinsic in the  $\beta$  term which is equal to the electrical power dissipation of a resistance divided by its volume times the thermal conductivity of the material (polysilicon in this case). The solution for this homogeneous second order differential equation (2) leads to the general solution:

$$T(x) = c_1 e^{\gamma x} + c_2 e^{-\gamma x} + \varepsilon \quad (3)$$

Here  $\varepsilon$  is:

$$\varepsilon = \frac{\beta + \gamma^2 T_\infty}{\gamma^2} \quad (4)$$

Equation 3 represents the temperature distribution along any of the four single elements defined in Fig. 2. Three more equations are obtained for the bimorph, cold and flexure elements. In this case, energy conservation conditions were applied to nodes a, b, and c. Temperature and heat transfer of the hot arm and the bimorph elements are the same at node a. Temperature and heat transfer of the bimorph part

and the cold arm are the same at node b, and the same applies to the cold arm and the flexure at node c. These equations of energy conservation can be summarized using a subscript  $e(i)$  to represent the element number. For example; the hot arm is the first element, the bimorph element is the second, and so forth. The  $j$  superscript represents the node number as shown in figure 2.

$$T_{e(i)}^j = T_{e(i+1)}^j \quad (5)$$

$$-kA_i \frac{dT_{e(i)}(x)}{dx} = -kA_{(i+1)} \frac{dT_{e(i+1)}(x)}{dx} \quad (6)$$

Here  $k$  is the thermal conductivity of the material;  $A$  is the area of the corresponding element, and  $T$  is the temperature at certain distance, which in this case is at node  $j$ .

The last two boundary conditions are related to the initial temperature at the anchored ends of the DTA.

$$T_{e1}(0) = c_1 + c_2 + \varepsilon_1 = T_0 \quad (7)$$

$$T_{e4}(L_t) = c_5 e^{\gamma_4 L_4} + c_6 e^{-\gamma_4 L_4} + \varepsilon_4 = T_0 \quad (8)$$

In solving these set of equations for each of the seven cases in which the ratio between the lateral thermal actuator side vs. the bimorph side increases, we obtained temperature distribution.

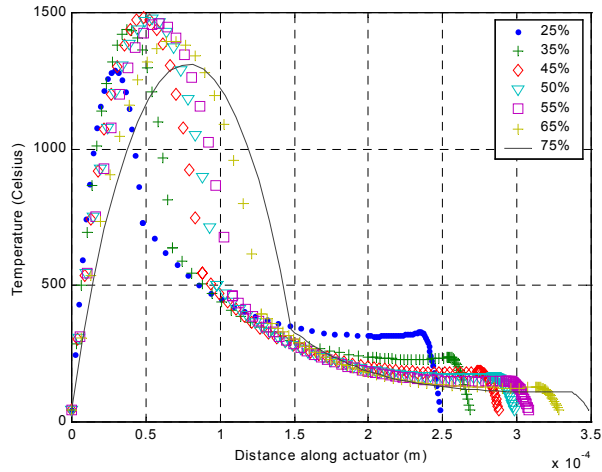


Fig 3. Temperature distribution predicted by the analytical model for seven different DTA designs.

The maximum temperatures for each design, all of them approximately located at the middle of the hot arm are shown in figure 4. These curves have different behavior as the result of an overlooked variable. Analytically we should

expect a decrease in temperature of the hot arms as it becomes longer, but this is not the case. While developing the analytical model the fact that the gap, between the structure layer (polysilicon 2) and the substrate, varies under the bimorph side was not considered. Further, analysis is recommended as future work considering the solution of a system of partial differential equations. Nevertheless, the displacements analytically obtained show unpredictable accuracy between analytical and numerical models.

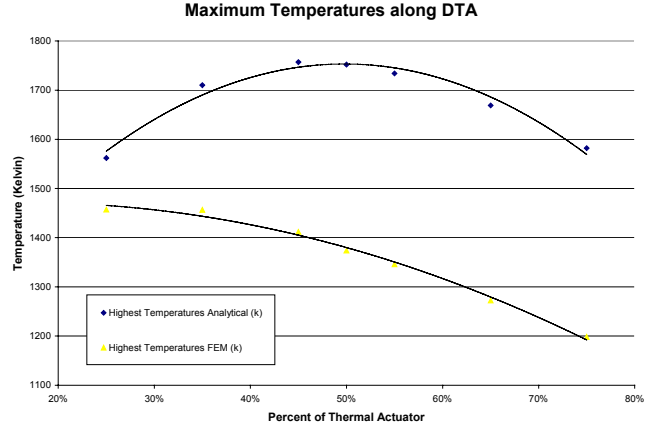


Fig 4. Comparison between predicted maximum temperatures along the DTA and the FEM results. Maximum temperatures located at the hot arm.

This temperature distribution was then used, together with equation 1, to calculate the lateral displacement where the hot and cold arms are connected with the bimorph element, which we'll call  $d_l$ . The actual lateral displacement of this actuator at its tip,  $d_r$ , is the addition of the displacement determined by using equation 1 and the additional displacement given by the extension of the bimorph element,  $d_2$ . These two displacements can be determined using the following equations;

$$d_1 = L_m \left( \frac{L_H}{\delta} + 1 \right) \left( 1 - \cos \left( \frac{\delta}{L_m} \right) \right) \quad (9)$$

where  $L_m$  is the distance from the center of the hot arm to the center of the gap between the arms multiply by 2,  $L_h$  is the total length of the hot arm before voltage been applied, and  $\delta$  is the thermal expansion of the element. The additional lateral displacement can easily be determined geometrically as;

$$d_2 = \frac{L_{morph} \delta}{L_m} \quad (10)$$

$$d_t = d_1 + d_2 \quad (11)$$

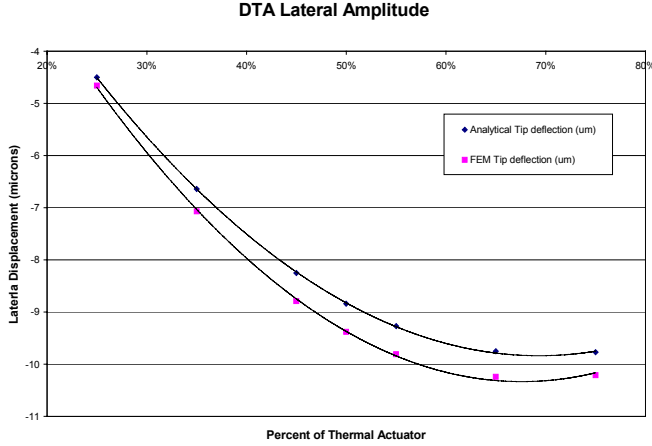


Fig 5. Lateral deflections predicted by the analytical model compared to the displacements predicted by the finite element FEM model

The other section of the DTA is the bimorph side. This section is, basically, two materials of the same length and different thermal coefficient of expansion, with constant cross section along beam, stacked together. Classical bimorph cantilever beam theory can then be applied without major changes. The bimorph beam theory, previously developed by others [6], has the following conditions: there is no internal friction between the bimorph layers, and the neutral axis of the bimorph beam lies on the common surface contact area. The temperature and material properties were assumed to be constant only and throughout this bimorph side with respect to time. The curvature due to thermal expansion mismatch is obtained from bimorph beam theory [6] to be;

$$k = \frac{6b_1b_2E_1E_2t_1t_2(t_1+t_2)(\alpha_1+\alpha_2)\Delta T}{(b_1E_1t_1^2)^2 + (b_2E_2t_2^2)^2 + 2b_1b_2E_1E_2t_1t_2(2t_1^2 + 3t_1t_2 + 2t_2^2)} \quad (12)$$

where  $E$  is Young's modulus,  $\alpha$  the coefficient of thermal expansion,  $b$  is the width,  $t$  is the thickness of the layers, and  $\Delta T$  is the change in temperature between the ambient and the stacked layers. The vertical deflection at the tip of a bimorph side is given by;

$$d_{vertical} = \frac{kL^2}{2} \quad (13)$$

where  $k$  is the already determined curvature of the bimorph beam and  $L$  is the length of only the bimorph side of the DTA.

Combining equation 11 and 13 and assuming an ambient temperature of 315 degrees Kelvin the FEM models can be compared. Figures 5 and 6 show accurate results between these models for each design.

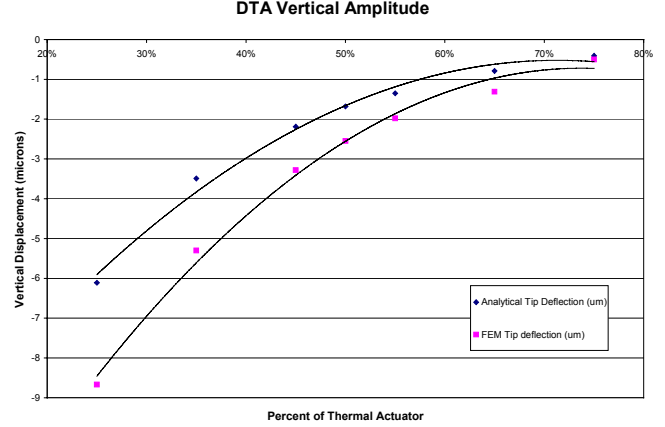


Fig 6. Vertical deflections predicted by the analytical model compared to the displacements predicted by the finite element FEM model

## Finite Element Modeling

The main limitation of the analytical model is that it does not consider a variable gap under the bimorph side of the DTA. Despite this limitation the analytical model shown reasonable accurate results in vertical and lateral displacements. Apparently, this overlooked variable did not affect the main purpose of this research, the optimization of amplitude. A finite element model was constructed to perform more detailed analysis of the temperature distribution along the actuator.

The commercial finite element package design specifically for MEMS design, MEMCAD was used to perform the analysis. The mesh consisted of stacked layers of 27-node solid elements with thickness that corresponded to the actual second structural layer of polysilicon.

The material properties were assumed to be constant but the coefficient of thermal expansion of polysilicon. The modeling/simulation consisted of an electro-mech-thermal analysis at constant voltage to obtain the vertical and lateral displacements.

## Analysis

A common situation with many bimorph microactuators is a non-zero tip displacement at room temperature after release. This is due to a thermal expansion mismatch of different deposited materials. Approximately 1.89  $\mu\text{m}$  deflection results once the metal layer (gold film) and the polysilicon layer reaches a steady state temperature (317 K). This displacement due to residual stress was not considered to simplify this analysis.

When electric current is initially supplied through the hot arm and then flows to both in-series thermo actuators. In the lateral side, the current density is higher through the thin elements, resulting in an expansion of the hot arm (figure 2) due to an ohmic heating. The bimorph side of the device curls when a resistive heating is induced by electrical power [4]. This curl actuation effect is due to the longer expansion of the stacked gold layer over polysilicon. The combination of these two different thermal effects will cause the tip to deflect laterally and vertically.

This bi-plane thermal actuator is a promising MEMS device that will lead to many applications such as micro-manipulation, nanofabrication and microrobots. The DTA is designed to be fabricated in MUMPs process and combines two thermal actuation mechanisms to operate in two space planes. An analytical model was developed to characterize the amplitude behavior of this device. Finite element modeling was performed to determine the right temperature distribution along the actuator and give insights of possible overlooked variables. Both analytical and numerical finite element models will be verified with experimental data.

- [1] Jeffrey T. Butler and Victor M. Bright. *Electrothermal and Fabrication Modeling of Polysilicon Thermal Actuators*. DSC-Vol. 66, Micro-Electro-Mechanical Systems (MEMS). ASME 1998
- [2] Bright, Victor. *Micro-Electro-Mechanical Systems*. University of Colorado at Boulder. 1999.
- [3] Kovacs, Gregory. *Micromachined Transducers Sourcebook*. McGraw-Hill Series, 1998. pp. 276-330. .
- [4] L-A. Liew, A. Tuantranont, V. M. Bright. *Modeling of thermal actuation in a bulk-micromachined CMOS micromirror*. Micro-electronics Journal 00 (2000). Pending for publishing.
- [5] John H. Comtois, Victor M. Bright, & Mark W. Phipps. *Thermal microactuators for surface-micromachining processes*, Proc. SPIE 2642 (1995) 10-21.
- [6] W.H. Chu, M. Mehregany & R.L. Mullen, *Analysis of tip deflection and force of a bimetallic cantilever microactuator*, Journal Micromech. microeng. 3 (1993) pp. 4-7.
- [7] Massood Tabid-Azar & Morton Litt. *Silicon Wafer-Scale micro-fabrication factory using scanning probe micro-robots*. Poster. Fifth Foresight Conference on Molecular Nanotechnology, 1997.
- [8] Sarita Thakoor. *Development of small, mobile, special-purpose robots*. Nasa Tech Brief, New Technology Report. Vol. 22, No. 2, Item #109 (1998) 1-15.
- [9] Paul Kladitis. Analytical modeling of a thermal actuator. Non published work, 2000. University of Colorado at Boulder. Dept. of Mechanical Engineering.

## References